Dedicated to Marius Tucsnak on the occasion of his 60^{th} *anniversary*

A CLASS OF SOLUTIONS FOR THE GRAPHENE HAMILTONIAN OPERATOR

C. CONCA, J. SAN MARTÍN, and V. SOLANO

Communicated by Sorin Micu

The graphene is a substance with carbon atoms arranged in a honeycomb lattice. The dynamics of the electrons in the structure is governed by the Hamilton equations of the system in the form of its associated spectral problem: $\mathcal{H}\Psi = \lambda\Psi$, with the additional condition that the eigenfunction Ψ must satisfy the so-called Kirchhoff's conditions. In this paper, we study a class of solutions (λ, Ψ) that, in addition to meeting these conditions, are periodic in one of the two main directions of the lattice, and satisfy a pseudo-periodicity type like condition in the other direction. Our main results lead to an adequate characterization of the dispersion relationships of the honeycomb lattice, providing a precise description of the regions of stability and instability of the eigenfunctions in terms of λ. As a consequence, a tool is thus obtained for a better understanding of the propagation properties and the behavior of the wave function of electrons in a hexagonal lattice, a key issue in graphene-based technologies.

AMS 2010 Subject Classification: 49J20.

Key words: periodic solutions, stability, general spectral theory, spectral theory, eigenvalue problems, graphene, honeycomb structure.

1. INTRODUCTION

Graphene is a novel material with carbon atoms arranged in a honeycomb lattice. The atomic composition of graphene corresponds to carbon atoms distributed over a single layer one atom thick. The superposition of several layers of graphene make up what is called the graphite material. Thus, graphene is an inherently two-dimensional material. In the past few years it has caught the attention of the scientific community for its peculiar electronic and mechanical properties and broad range of applications [2, 5, 10, 15, 16, 25]. To be able to predict and improve the understanding of these properties, mathematical models are not only useful but necessary. This has been approached from different scientific fields such as quantum networks (*e.g.*, [4, 17, 18, 20])), also called quantum graphs, in chemistry [23, 24] and physics [2, 5, 10, 21, 22].

The dynamics of the electrons in the lattice can be captured by solving the Hamilton equations of the system as a spectral problem $\mathcal{H}\Psi = \lambda\Psi$, with the extra condition that the eigenfunction Ψ must be a feasible solution in the sense that it satisfies the so-called Kirchhoff's conditions (see (13), (14) in Section 1.1.2). Although a full characterization of the set of feasible solutions stands as an open mathematical challenge, this paper partially addresses this question through the study of a class of feasible solutions (λ, Ψ), which are periodic in one of the two main directions of the honeycomb lattice (see (28)), while satisfying a pseudo-periodicity condition in the other one (see (27)). This latter condition, which depends on a complex parameter ρ, is central when classifying solutions as stable (or bounded) and unstable (or unbounded), as previously done in [3] for a one-dimensional system in $\mathbb{R}$, and later generalized to $\mathbb{R}^2$ in [8, 9].

Our main result (Theorem 4) shows that for every $\lambda \in \mathbb{R}$ there exists $\rho \in \mathbb{C}$, and feasible periodic solutions of $\mathcal{H}\Psi = \lambda\Psi$, which also meet the pseudo-periodicity condition for ρ. For each fixed λ, this theorem also makes explicit the corresponding values of ρ through the so-called dispersion relationships; Table 1 summarizes these relations in terms of λ, which are obtained from the solution of the energy eigenvalue problem given by the lattice Hamiltonian. As a corollary of the information contained herein, a detailed analysis follows on the behavior of the eigenfunctions in terms of λ, which precise those values of λ giving rise to bounded or unbounded eigenfunctions in the vertical direction, and those that generate both types of solutions. A proper characterization of the dispersion relations of the honeycomb lattice is of particular interest for exploiting graphene electronic properties. More precisely, our systematic study of such stability and instability regions provides a tool to understand the propagation properties and behavior of the electrons wave-function in a hexagonal lattice, a key question in graphene-based technologies.

To conclude, let us mention some relationships between this paper and the vast existing physical-mathematical literature on differential operators in infinite graphs. Using techniques similar to those used here, electromagnetic waves that propagate through a periodic honeycomb lattice are studied in [1]. Our eigenfunction stability results generalize those obtained using the quantum graph model introduced in [19], and recently studied by different authors [6, 7, 13, 26], which is based on the one-dimensional techniques of Floquet's theory on periodic solutions [14]. An analysis that could shed new light on all these interesting theoretical and applied questions would be to carry out a comparative study with the alternative approach introduced in [12].

The paper is organized in the following manner. As part of this Introduction, in Section 1.1 we summarize some previous results on this topic and establish basic notations. Then Section 1.2 is devoted to presenting new results, in particular, a new class of solutions for our spectral problem $\mathcal{H}\Psi = \lambda\Psi$, and its splitting into stable and unstable solutions. We conclude with Section 2, where these results are proved.

1.1. **Survey of the previous results**

The mathematical definition of the problem has been set in previous works [9]. However, here we summarize theorems and definitions necessaries to present our current results.

1.1.1. **Floquet theory**

Let us consider the Hill's equation defined in [11] as

$$-\Psi''(x) + V(x)\Psi(x) = \lambda\Psi(x). \tag{1}$$

Here, V is real $L^2(0,1)$ function, which is assumed to also be piecewise-continuous and 1-periodic. We know that equation (1) has a basis of two linearly independent solutions $\varphi_1(\cdot;\lambda)$ and $\varphi_2(\cdot;\lambda)$, functions of the parameter λ, defined by:

$$\begin{cases} -\varphi_1''(x;\lambda) + V(x)\varphi_1(x;\lambda) = \lambda\varphi_1(x;\lambda) \\ \varphi_1(0;\lambda) = 1, \quad \varphi_1'(0;\lambda) = 0 \end{cases} \tag{2}$$

and

$$\begin{cases} -\varphi_2''(x;\lambda) + V(x)\varphi_2(x;\lambda) = \lambda\varphi_2(x;\lambda) \\ \varphi_2(0;\lambda) = 0, \quad \varphi_2'(0;\lambda) = 1. \end{cases} \tag{3}$$

It is clear that any solution Ψ of (1) can be written as a linear combination:

$$\Psi(x) = \Psi(0)\varphi_1(x;\lambda) + \Psi'(0)\varphi_2(x;\lambda). \tag{4}$$

To simplify matters, in what follows we will restrict our analysis to symmetric potentials in the sense that we will assume that V satisfies the relation

$$V(1-x) = V(x) \quad \text{for a.e. } x \in [0,1].$$

For such kind of potentials, it is straightforward proved that

$$\varphi_2'(1;\lambda) = \varphi_1(1;\lambda). \tag{5}$$

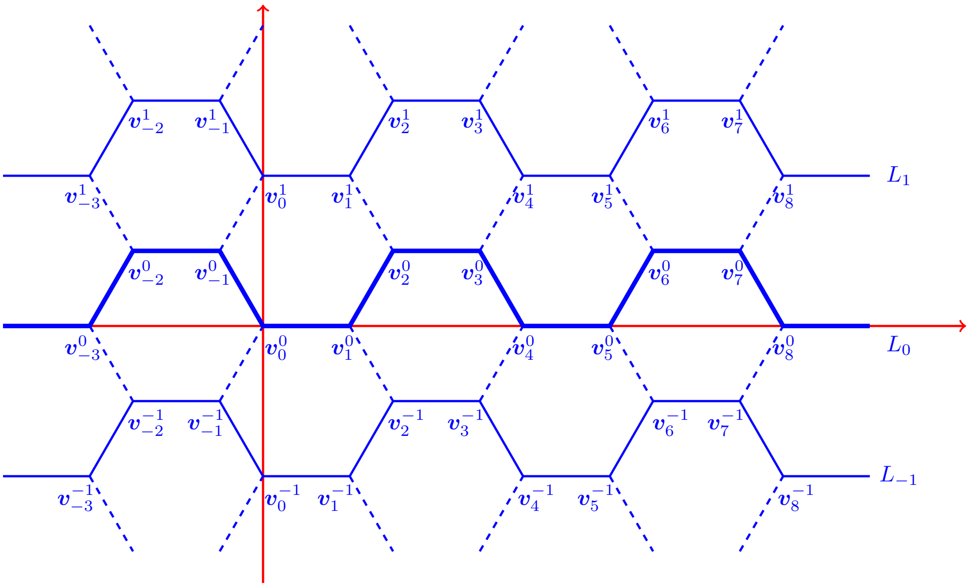

Fig. 1 – Vertices $\boldsymbol{v}_i^j$ and profiles L_j representing the graphene G.

1.1.2. **The graphene**

The graphene is a substance made of pure carbon, where the atoms follow a regular hexagon pattern. This atoms are mathematically described by a set of vertices $\mathcal{V} \subseteq \mathbb{R}^2$ as Figure 1 shows.

More precisely, denoting the canonical vectors

$$\boldsymbol{e}_1 = (1, 0) \qquad \text{y} \qquad \boldsymbol{e}_2 = (0, 1)\,, \tag{6}$$

the set of vertices $\mathcal{V}$ is defined by

$$\mathcal{V} = \left\{\boldsymbol{v}_i^j : i, j \in \mathbb{Z}\right\}, \tag{7}$$

where

$$\boldsymbol{v}_i^j = \begin{cases} \frac{3i}{4}\boldsymbol{e}_1 + j\sqrt{3}\boldsymbol{e}_2 & \text{if } i = 4m,\ m \in \mathbb{Z},\ j \in \mathbb{Z} \\ \frac{3i+1}{4}\boldsymbol{e}_1 + j\sqrt{3}\boldsymbol{e}_2 & \text{if } i = 4m+1,\ m \in \mathbb{Z},\ j \in \mathbb{Z} \\ \frac{3i}{4}\boldsymbol{e}_1 + (j+\frac{1}{2})\sqrt{3}\boldsymbol{e}_2 & \text{if } i = 4m+2,\ m \in \mathbb{Z},\ j \in \mathbb{Z} \\ \frac{3i+1}{4}\boldsymbol{e}_1 + (j+\frac{1}{2})\sqrt{3}\boldsymbol{e}_2 & \text{if } i = 4m+3,\ m \in \mathbb{Z},\ j \in \mathbb{Z} \end{cases} \tag{8}$$

As Figures 1 and 2 show, these vertices are connected by a set of edges

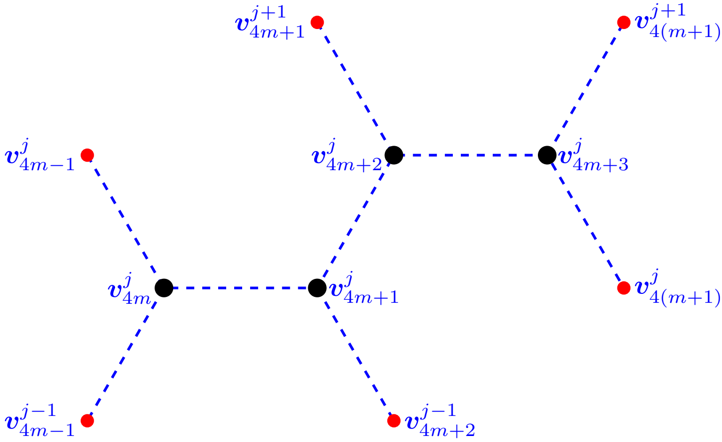

Fig. 2 – Edges $[\boldsymbol{v}^j_i, \boldsymbol{v}^j_{i+1}]$ connecting the vertices of the same profile L_j and edges which connect adjacent profiles.

$\mathcal{A}$ defined by

$$\begin{aligned}\mathcal{A} = \Big\{[\boldsymbol{v}^j_i, \boldsymbol{v}^j_{i+1}] : i, j \in \mathbb{Z}\Big\} \bigcup \Big\{&[\boldsymbol{v}^j_{4m}, \boldsymbol{v}^{j-1}_{4m-1}], [\boldsymbol{v}^j_{4m+1}, \boldsymbol{v}^{j-1}_{4m+2}], \\ &[\boldsymbol{v}^j_{4m+2}, \boldsymbol{v}^{j+1}_{4m+1}], [\boldsymbol{v}^j_{4m+3}, \boldsymbol{v}^{j+1}_{4(m+1)}] : m, j \in \mathbb{Z}\Big\}.\end{aligned} \tag{9}$$

These set of edges and vertices constitute an hexagonal grid. Using this notation, the structure of the graphene is represented by a non-oriented graph G determined by the set of vertices and edges previously defined, *i.e.*,

$$G = (\mathcal{V}, \mathcal{A}).$$

We notice that each edge of the graphene is bijective to the segment $[0, 1] \subseteq \mathbb{R}$. In fact, in order to visualize this bijection, we consider the parameterization $\boldsymbol{\sigma}$, oriented from $\boldsymbol{v}$ to $\boldsymbol{w}$, defined by:

$$\begin{array}{rcl}\boldsymbol{\sigma} : [0, 1] \times \mathbb{R}^2 \times \mathbb{R}^2 & \to & \mathbb{R}^2 \\ (t; \boldsymbol{v}, \boldsymbol{w}) & \mapsto & \boldsymbol{\sigma}(t; \boldsymbol{v}, \boldsymbol{w}) = \boldsymbol{v} + t(\boldsymbol{w} - \boldsymbol{v}).\end{array} \tag{10}$$

Thus, each edge $[\boldsymbol{v}_1, \boldsymbol{v}_2] \in \mathcal{A}$ can be written as $\boldsymbol{\sigma}([0, 1]; \boldsymbol{v}_1, \boldsymbol{v}_2)$. The inverse function is such that

$$\mathbf{x} \in [\boldsymbol{v}_1, \boldsymbol{v}_2] \mapsto \boldsymbol{\sigma}^{-1}(\mathbf{x}; \boldsymbol{v}_1, \boldsymbol{v}_2) = \frac{\| \mathbf{x} - \boldsymbol{v}_1 \|}{\| \boldsymbol{v}_2 - \boldsymbol{v}_1 \|}. \tag{11}$$

Using (10), whose inverse is (11), for each edge $[\boldsymbol{v}_1, \boldsymbol{v}_2] \in \mathcal{A}$ we can define the space $L^2(\boldsymbol{v}_1, \boldsymbol{v}_2)$ as follows:

$$L^2(\boldsymbol{v}_1, \boldsymbol{v}_2) = \Big\{\Psi_{[v_1, v_2]} := \widetilde{\Psi} \circ \boldsymbol{\sigma}^{-1}(\cdot; \boldsymbol{v}_1, \boldsymbol{v}_2) : \widetilde{\Psi} \in L^2(0, 1)\Big\},$$

endowed with the norm $\|\Psi_{[v_1,v_2]}\|_{L^2(\boldsymbol{v}_1,\boldsymbol{v}_2)} = \|\widetilde{\Psi}\|_{L^2(0,1)}$. Then, we can define $\mathcal{W}(\mathcal{A})$ as:

$$\mathcal{W}(\mathcal{A}) = \Big\{(\Psi_a)_{a\in\mathcal{A}} \in \bigotimes_{a\in\mathcal{A}} L^2(a)\Big\}. \tag{12}$$

This space can be also called $\mathcal{W}(G)$; it is an infinite dimensional linear space.

Similarly, for each edge $[\boldsymbol{v}_1, \boldsymbol{v}_2] \in \mathcal{A}$ we can define the Sobolev space $H^2(\boldsymbol{v}_1, \boldsymbol{v}_2)$ by:

$$H^2(\boldsymbol{v}_1, \boldsymbol{v}_2) = \Big\{\Psi_{[v_1,v_2]} := \widetilde{\Psi} \circ \boldsymbol{\sigma}^{-1}(\cdot; \boldsymbol{v}_1, \boldsymbol{v}_2) : \widetilde{\Psi} \in H^2(0,1)\Big\},$$

endowed with the norm $\|\Psi_{[v_1,v_2]}\|_{H^2(\boldsymbol{v}_1,\boldsymbol{v}_2)} = \|\widetilde{\Psi}\|_{H^2(0,1)}$. Thus, the Sobolev space $\mathcal{W}^2(G)$ is defined as the subset of functions $(\Psi_a)_{a\in\mathcal{A}} \in \bigotimes_{a\in\mathcal{A}} H^2(a)$ which satisfy the two following conditions:

$$\forall \boldsymbol{v} \in \mathcal{V}, \forall a_1, a_2 \in \mathcal{A}\ [\boldsymbol{v} \in a_1 \cap a_2 \Rightarrow \Psi_{a_1}(\boldsymbol{v}) = \Psi_{a_2}(\boldsymbol{v})], \tag{13}$$

$$\forall \boldsymbol{v} \in \mathcal{V} \sum_{\substack{\boldsymbol{v}_2\in\mathcal{V} \\ [\boldsymbol{v},\boldsymbol{v}_2]\in\mathcal{A}}} D\Psi_{[\boldsymbol{v},\boldsymbol{v}_2]}(\boldsymbol{v}; \boldsymbol{v}_2 - \boldsymbol{v}) = 0, \tag{14}$$

where we have denoted by $D\Psi_{[\boldsymbol{v},\boldsymbol{v}_2]}(\boldsymbol{v}; \boldsymbol{v}_2 - \boldsymbol{v})$ the directional derivative of the function $\Psi_{[\boldsymbol{v},\boldsymbol{v}_2]}$ at the point $\boldsymbol{v}$ in the direction $\boldsymbol{v}_2 - \boldsymbol{v}$. These conditions are usually called Kirchhoff's conditions of the graphene structure. The first of these conditions, (13), corresponds to the continuity condition on each vertex going from one edge to the other. The second one, (14), states that the sum of the outward fluxes from each vertex $\boldsymbol{v}$ must be zero.

1.1.3. **The graphene Hamiltonian operator**

The Hamiltonian of graphene is the operator $\mathcal{H} : \mathcal{D}(\mathcal{H}) \subset \mathcal{W}(G) \to \mathcal{W}(G)$, with domain $\mathcal{D}(\mathcal{H}) = \mathcal{W}^2(G)$, that maps $\Psi = (\Psi_a)_{a\in\mathcal{A}} \in \mathcal{W}^2(G)$ to $\mathcal{H}\Psi \in \mathcal{W}(G)$, $\mathcal{H}\Psi = ((\mathcal{H}\Psi)_a)_{a\in A}$, such that

$$(\mathcal{H}\Psi)_a(\mathbf{x}) = \Big(-\widetilde{\Psi}_a'' + V\widetilde{\Psi}_a\Big) \circ \boldsymbol{\sigma}^{-1}(\mathbf{x}; a), \tag{15}$$

where, for each edge $a \in \mathcal{A}$, $\widetilde{\Psi}_a = \Psi_a \circ \boldsymbol{\sigma}(\cdot; a) \in H^2(0,1)$.

The goal of this section is to study the spectrum of the operator $\mathcal{H}$, characterizing the functions Ψ which are bounded or unbounded solutions. In order to do this, we seek for non-zero functions $\Psi = (\Psi_a)_{a\in\mathcal{A}}$ satisfying (13)–(14) and the following differential equations

$$-\widetilde{\Psi}_a''(t) + V(t)\widetilde{\Psi}_a(t) = \lambda\widetilde{\Psi}_a(t), \quad \forall a \in \mathcal{A}, \forall t \in (0,1), \tag{16}$$

where $\lambda \in \mathbb{R}$ is a parameter.

1.1.4. **A mathematical basis for the graphene**

Taking into account the hexagonal periodic geometry of the graphene, the Kirchhoff's conditions (13), (14) have been written in Theorems 1 and 2 of [8]. Each of these theorems distinguishes between the cases $\varphi_2(1;\lambda) \neq 0$ and $\varphi_2(1;\lambda) = 0$, where $\varphi_2(\cdot;\lambda)$ is the function defined in (2). With the notations of this paper, these are rephrased as follows:

THEOREM 1. *If $\varphi_2(1;\lambda) \neq 0$, then every function $\Psi = (\Psi_a)_{a\in\mathcal{A}}$ satisfying* (16), *also satisfies the equations (13)–(14) if and only if, for each $m, j \in \mathbb{Z}$, it holds*

$$\begin{array}{llcl}
(17) & \Psi(\boldsymbol{v}^j_{4m}) - 3\varphi_1(1;\lambda)\Psi(\boldsymbol{v}^j_{4m+1}) + \Psi(\boldsymbol{v}^j_{4m+2}) + \Psi(\boldsymbol{v}^{j-1}_{4m+2}) & = & 0 \\
(18) & \Psi(\boldsymbol{v}^{j+1}_{4m+1}) + \Psi(\boldsymbol{v}^j_{4m+1}) - 3\varphi_1(1;\lambda)\Psi(\boldsymbol{v}^j_{4m+2}) + \Psi(\boldsymbol{v}^j_{4m+3}) & = & 0 \\
(19) & \Psi(\boldsymbol{v}^j_{4m+2}) - 3\varphi_1(1;\lambda)\Psi(\boldsymbol{v}^j_{4m+3}) + \Psi(\boldsymbol{v}^j_{4(m+1)}) + \Psi(\boldsymbol{v}^{j+1}_{4(m+1)}) & = & 0 \\
(20) & \Psi(\boldsymbol{v}^{j-1}_{4m+3}) + \Psi(\boldsymbol{v}^j_{4m+3}) - 3\varphi_1(1;\lambda)\Psi(\boldsymbol{v}^j_{4(m+1)}) + \Psi(\boldsymbol{v}^j_{4(m+1)+1}) & = & 0
\end{array}$$

where $\varphi_1(\cdot;\lambda)$ and $\varphi_1(\cdot;\lambda)$ are the functions defined in (2)–(3).

THEOREM 2. *If $\varphi_2(1;\lambda) = 0$, every function $\Psi = (\Psi_a)_{a\in\mathcal{A}}$ satisfying* (16), *also satisfies the equations* (13)–(14) *if and only if the following conditions hold:*

(1) *There exists $k_\Psi \in \mathbb{R}$, depending on Ψ, such that*

$$(21) \qquad \Psi(\boldsymbol{v}^j_{2m}) = k_\Psi \quad \text{and} \quad \Psi(\boldsymbol{v}^j_{2m-1}) = k_\Psi \varphi_1(1;\lambda), \quad \forall m, j \in \mathbb{Z}.$$

(2) *If on each edge $a \in \mathcal{A}$ the functions Ψ_a can be written as*

$$(22) \qquad \widetilde{\Psi}_a(t) = \widetilde{\Psi}_a(0)\varphi_1(t;\lambda) + c_a\varphi_2(t;\lambda),$$

where the parameterization t is chosen such that the edge goes from left to right, then the constants $(c_a)_{a\in\mathcal{A}}$ satisfy the relations:

$$(23) \quad 2k_\Psi\varphi_1'(1;\lambda) + c_{[\boldsymbol{v}^j_{4m-1},\boldsymbol{v}^j_{4m}]} + c_{[\boldsymbol{v}^{j-1}_{4m-1},\boldsymbol{v}^j_{4m}]} = c_{[\boldsymbol{v}^j_{4m},\boldsymbol{v}^j_{4m+1}]}\varphi_1(1;\lambda), \quad \forall m, j \in \mathbb{Z},$$

$$(24) \quad k_\Psi\varphi_1'(1;\lambda) + c_{[\boldsymbol{v}^j_{4m},\boldsymbol{v}^j_{4m+1}]}\varphi_1(1;\lambda) = c_{[\boldsymbol{v}^j_{4m+1},\boldsymbol{v}^j_{4m+2}]} + c_{[\boldsymbol{v}^j_{4m+1},\boldsymbol{v}^{j-1}_{4m+2}]}, \quad \forall m, j \in \mathbb{Z},$$

$$(25) \quad 2k_\Psi\varphi_1'(1;\lambda) + c_{[\boldsymbol{v}^j_{4m+1},\boldsymbol{v}^j_{4m+2}]} + c_{[\boldsymbol{v}^{j+1}_{4m+1},\boldsymbol{v}^j_{4m+2}]} = c_{[\boldsymbol{v}^j_{4m+2},\boldsymbol{v}^j_{4m+3}]}\varphi_1(1;\lambda), \quad \forall m, j \in \mathbb{Z},$$

$$(26) \quad k_\Psi\varphi_1'(1;\lambda) + c_{[\boldsymbol{v}^j_{4m+2},\boldsymbol{v}^j_{4m+3}]}\varphi_1(1;\lambda) = c_{[\boldsymbol{v}^j_{4m+3},\boldsymbol{v}^j_{4(m+1)}]} + c_{[\boldsymbol{v}^j_{4m+3},\boldsymbol{v}^{j+1}_{4(m+1)}]}, \quad \forall m, j \in \mathbb{Z}.$$

Based upon Theorem 1, in [8] it is shown that the set of vertices that belong to any profile $L_j = \{\boldsymbol{v}_i^j : i \in \mathbb{Z}\}$ forms a basis for the graphene solutions in the sense of [8, Proposition 1], that is

Proposition 1. *Let $\Psi \in \mathcal{W}(G)$ such that $\mathcal{H}\Psi \equiv \lambda\Psi$. If, for a given $q \in \mathbb{Z}$, the values of Ψ at the vertices of L_q are known, then the value of Ψ at every vertex and edge of G can be uniquely determined.*

1.2. **Presentation of new results: Periodic feasible solutions**

Using the geometry introduced in [8] and the results obtained in [9], in this paper we are interested in studying the existence of solutions of $\mathcal{H}\Psi \equiv \lambda\Psi$ that satisfy the supplementary condition

$$\Psi(\boldsymbol{x} + \sqrt{3}\boldsymbol{e}_2) = \rho\Psi(\boldsymbol{x}) \qquad \forall \boldsymbol{x} \in G \tag{27}$$

where ρ is a non zero real or complex number.

Our main results in this sense are stated in the following two theorems. In the former one, the existence of solutions that meet the vertical growth condition given by (27) is studied. Given that there are infinitely many solutions that satisfy this condition, in Theorem 4 we look for those that furthermore, they are periodic in the horizontal direction.

Theorem 3. *For every $\lambda \in \mathbb{R}$ such that $\varphi_2(1;\lambda) \neq 0$ and for all $\rho \in \mathbb{C} \setminus \{-1\}$, the solutions of $\mathcal{H}\Psi \equiv \lambda\Psi$, which also satisfy the condition (27), form a vector space of dimension 2.*

Theorem 4. *For every $\lambda \in \mathbb{R}$ there exists $\rho \in \mathbb{C} \setminus \{-1\}$ and solutions of $\mathcal{H}\Psi \equiv \lambda\Psi$ satisfying (27), and which are additionally periodic in the following sense:*

$$\Psi(\boldsymbol{v}_{i+4}^j) = \Psi(\boldsymbol{v}_i^j) \quad \forall i, j \in \mathbb{Z}. \tag{28}$$

Moreover, if for each $\lambda \in \mathbb{R}$, an auxiliary variable $z(\lambda)$ is introduced taking the values $z_1(\lambda)$ or $z_2(\lambda)$, defined by

$$z_{1,2}(\lambda) = \Big(3\varphi_1(1;\lambda) \pm 1\Big)^2, \tag{29}$$

then the values of ρ are obtained as a function of $z(\lambda)$ as follows

$$\rho(z)_{1,2} = \frac{z - 2 \pm \sqrt{(z-4)z}}{2}, \tag{30}$$

and they satisfy $\rho_1\rho_2 = 1$. Depending on whether $z(\lambda) \geq 4$ or $z(\lambda) < 4$, we get that ρ is real, or ρ is a unitary complex number, say $\rho = e^{\pm i\theta}$, with

$$\theta = \arccos\Big(\frac{z(\lambda) - 2}{2}\Big).$$

Table 1 summarizes all possible cases, based on the values of $\varphi_1(1;\lambda)$.

Finally, if $\varphi_1(1;\lambda) \neq 0$*, at the vertices* $\boldsymbol{v}^j_{4m}, \boldsymbol{v}^j_{4m+1}, \boldsymbol{v}^j_{4m+2}, \boldsymbol{v}^j_{4m+3}$*, the solutions* Ψ *associated with* z_1 *or* z_2 *take, respectively, the values given by the following valued-vectors:*

$$\begin{bmatrix}\Psi(\boldsymbol{v}^j_{4m})\\ \Psi(\boldsymbol{v}^j_{4m+1})\\ \Psi(\boldsymbol{v}^j_{4m+2})\\ \Psi(\boldsymbol{v}^j_{4m+3})\end{bmatrix} = \begin{bmatrix}1\\ 1\\ s_1\cdot\sqrt{\rho}\\ s_1\cdot\sqrt{\rho}\end{bmatrix}\Psi(\boldsymbol{v}^j_{4m}) \quad \textit{and} \quad \begin{bmatrix}\Psi(\boldsymbol{v}^j_{4m})\\ \Psi(\boldsymbol{v}^j_{4m+1})\\ \Psi(\boldsymbol{v}^j_{4m+2})\\ \Psi(\boldsymbol{v}^j_{4m+3})\end{bmatrix} = \begin{bmatrix}1\\ -1\\ -s_2\cdot\sqrt{\rho}\\ s_2\cdot\sqrt{\rho}\end{bmatrix}\Psi(\boldsymbol{v}^j_{4m}) \tag{31}$$

where

$$s_1 = \begin{cases}1 & \textit{if } \varphi_1(1;\lambda) > 1/3\\ -1 & \textit{if } \varphi_1(1;\lambda) < 1/3\end{cases} \quad \textit{and} \quad s_2 = \begin{cases}1 & \textit{if } \varphi_1(1;\lambda) > -1/3\\ -1 & \textit{if } \varphi_1(1;\lambda) < -1/3\end{cases}. \tag{32}$$

$\varphi_1(1;\lambda)$	$\rho(z_1)$	$\rho(z_2)$
$\in (-\infty,-1)$	$\rho_{1,2}\in\mathbb{R},\ 0<\rho_1<1<\rho_2$	$\rho_{1,2}\in\mathbb{R},\ 0<\rho_1<1<\rho_2$
$=-1$	$\rho_1=\rho_2=1$	$\rho_{1,2}\in\mathbb{R},\ 0<\rho_1<1<\rho_2$
$\in(-1,-1/3)$	$\rho_{1,2}=e^{\pm i\theta}$, $\cos\theta=\frac{(3\varphi_1(1;\lambda)+1)^2-2}{2}$	$\rho_{1,2}\in\mathbb{R},\ 0<\rho_1<1<\rho_2$
$=-1/3$	$=-1$ (excluded value)	$=1$
$\in(-1/3,1/3)$	$\rho_{1,2}=e^{\pm i\theta}$, $\cos\theta=\frac{(3\varphi_1(1;\lambda)+1)^2-2}{2}$	$\rho_{1,2}=e^{\pm i\theta}$, $\cos\theta=\frac{(3\varphi_1(1;\lambda)-1)^2-2}{2}$
$=1/3$	$=1$	$=-1$ (excluded value)
$\in(1/3,1)$	$\rho_{1,2}\in\mathbb{R},\ 0<\rho_1<1<\rho_2$	$\rho_{1,2}=e^{\pm i\theta}$, $\cos\theta=\frac{\left(3\varphi_1(1;\lambda)-1\right)^2-2}{2}$
$=1$	$\rho_{1,2}\in\mathbb{R},\ 0<\rho_1<1<\rho_2$	$=1$
$\in(1,\infty)$	$\rho_{1,2}\in\mathbb{R},\ 0<\rho_1<1<\rho_2$	$\rho_{1,2}\in\mathbb{R},\ 0<\rho_1<1<\rho_2$

Table 1 – Dependency of ρ in terms of λ, where $\varphi_1(1:\lambda)$ is the function defined in (2) and z_1, z_2 are defined in (29).

Remark 1. Figures 3–6 graph the solutions (31) for each of the four combinations of values $z = z_{1,2}$, $s_{1,2} = \pm 1$.

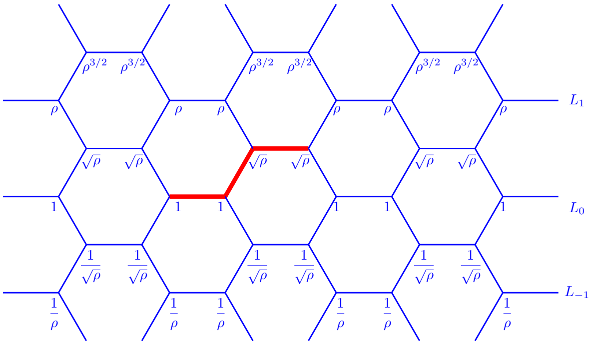

Fig. 3 – Graph of the solution of $\mathcal{H}\Psi \equiv \lambda\Psi$, which also satisfies (27), (28), in case $\varphi_1(1;\lambda) > 1/3$, $z = z_1$, and $\Psi(\boldsymbol{v}_{4m}^0) = 1$.

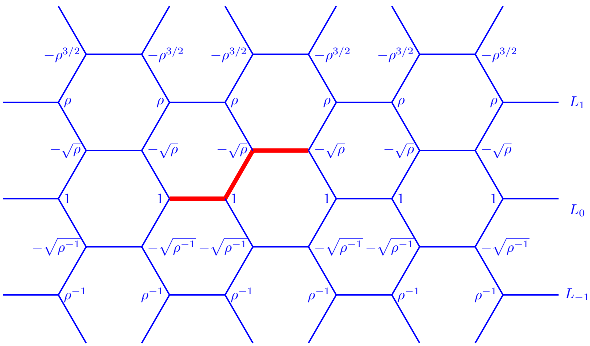

Fig. 4 – Graph of the solution of $\mathcal{H}\Psi \equiv \lambda\Psi$, which also satisfies (27), (28), in case $\varphi_1(1;\lambda) < 1/3$, $z = z_1$, and $\Psi(\boldsymbol{v}_{4m}^0) = 1$.

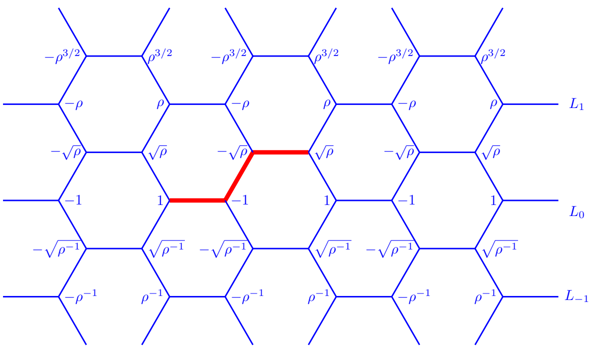

Fig. 5 – Graph of the solution of $\mathcal{H}\Psi \equiv \lambda\Psi$, which also satisfies (27), (28), in case $\varphi_1(1;\lambda) > -1/3$, $z = z_2$, and $\Psi(\boldsymbol{v}_{4m}^0) = 1$.

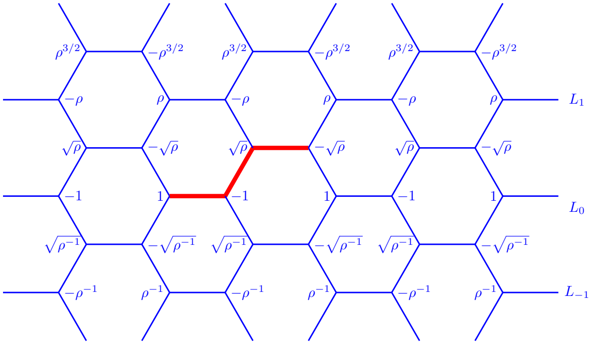

Fig. 6 – Graph of the solution of $\mathcal{H}\Psi \equiv \lambda\Psi$, which also satisfies (27), (28), in case $\varphi_1(1;\lambda) < -1/3$, $z = z_2$, and $\Psi(\boldsymbol{v}^0_{4m}) = 1$.

Corollary 1. i) *If* $|\varphi_1(1;\lambda)| > 1$, *all of the solutions of* $\mathcal{H}\Psi \equiv \lambda\Psi$, *satisfying conditions* (27), (28), *are unbounded in the vertical direction.*

ii) *If* $|\varphi_1(1;\lambda)| \leq 1/3$, *all of the solutions of* $\mathcal{H}\Psi \equiv \lambda\Psi$, *satisfying conditions* (27), (28), *are bounded in the vertical direction.*

iii) *If* $|\varphi_1(1;\lambda)| \in (1/3, 1]$, *then there is coexistence of solutions of* $\mathcal{H}\Psi \equiv \lambda\Psi$, *satisfying* (27), (28), *which are bounded and unbounded in the vertical direction.*

Theorem 5. *For every* $\lambda \in \mathbb{R}$ *such that* $\varphi_1(1;\lambda) = \pm 1/3$ *there exist solutions of* $\mathcal{H}\Psi \equiv \lambda\Psi$, *satisfying condition* (27) *with* $\rho = -1$, *and which are additionally periodic in the sense of* (28).

Moreover, if $\varphi_1(1;\lambda) = 1/3$, *at the vertices* $\boldsymbol{v}^j_{4m}, \boldsymbol{v}^j_{4m+1}, \boldsymbol{v}^j_{4m+2}, \boldsymbol{v}^j_{4m+3}$ *the solutions* Ψ *take the values given by the following valued-vectors:*

$$\begin{bmatrix}\Psi(\boldsymbol{v}^j_{4m})\\ \Psi(\boldsymbol{v}^j_{4m+1})\\ \Psi(\boldsymbol{v}^j_{4m+2})\\ \Psi(\boldsymbol{v}^j_{4m+3})\end{bmatrix} = \begin{bmatrix}1\\1\\0\\0\end{bmatrix}\Psi(\boldsymbol{v}^j_{4m}) + \begin{bmatrix}0\\0\\1\\1\end{bmatrix}\Psi(\boldsymbol{v}^j_{4m+1}), \tag{33}$$

where $\Psi(\boldsymbol{v}^j_{4m})$, $\Psi(\boldsymbol{v}^j_{4m+1})$ *are both arbitrary. In case* $\varphi_1(1;\lambda) = -1/3$ *these solutions are given by*

$$\begin{bmatrix}\Psi(\boldsymbol{v}^j_{4m})\\ \Psi(\boldsymbol{v}^j_{4m+1})\\ \Psi(\boldsymbol{v}^j_{4m+2})\\ \Psi(\boldsymbol{v}^j_{4m+3})\end{bmatrix} = \begin{bmatrix}1\\-1\\0\\0\end{bmatrix}\Psi(\boldsymbol{v}^j_{4m}) + \begin{bmatrix}0\\0\\1\\-1\end{bmatrix}\Psi(\boldsymbol{v}^j_{4m+1}), \tag{34}$$

where $\Psi(\boldsymbol{v}^j_{4m})$, $\Psi(\boldsymbol{v}^j_{4m+1})$ *are again arbitrary.*

2. PROOF OF THE MAIN RESULTS

Proof of Theorem 3. Since $\varphi_2(1;\lambda) \neq 0$, Kirchhoff's conditions for solutions of $\mathcal{H}\Psi \equiv \lambda\Psi$, which satisfy (27) for any profile L_j (see Figure 1), are written for each $m \in \mathbb{Z}$ as follows:

$$\Psi(\boldsymbol{v}^j_{4m}) - 3\varphi_1(1;\lambda)\Psi(\boldsymbol{v}^j_{4m+1}) + (1+\rho^{-1})\Psi(\boldsymbol{v}^j_{4m+2}) = 0 \tag{35}$$

$$(1+\rho)\Psi(\boldsymbol{v}^j_{4m+1}) - 3\varphi_1(1;\lambda)\Psi(\boldsymbol{v}^j_{4m+2}) + \Psi(\boldsymbol{v}^j_{4m+3}) = 0 \tag{36}$$

$$\Psi(\boldsymbol{v}^j_{4m+2}) - 3\varphi_1(1;\lambda)\Psi(\boldsymbol{v}^j_{4m+3}) + (1+\rho)\Psi(\boldsymbol{v}^j_{4(m+1)}) = 0 \tag{37}$$

$$(1+\rho^{-1})\Psi(\boldsymbol{v}^j_{4m+3}) - 3\varphi_1(1;\lambda)\Psi(\boldsymbol{v}^j_{4(m+1)}) + \Psi(\boldsymbol{v}^j_{4(m+1)+1}) = 0 \tag{38}$$

The above equations form an infinite tridiagonal linear system. Since $\rho \neq -1$, this system is straightforward solved in terms of $\Psi(\boldsymbol{v}^j_{4m})$, $\Psi(\boldsymbol{v}^j_{4m+1})$. Precisely, we have

$$\Psi(\boldsymbol{v}^j_{4m+2}) = \frac{-1}{(1+\rho^{-1})}\Psi(\boldsymbol{v}^j_{4m}) + \frac{3\varphi_1(1;\lambda)}{(1+\rho^{-1})}\Psi(\boldsymbol{v}^j_{4m+1}) \tag{39}$$

$$\begin{aligned}\Psi(\boldsymbol{v}^j_{4m+3}) = {} & \frac{-3\varphi_1(1;\lambda)}{(1+\rho^{-1})}\Psi(\boldsymbol{v}^j_{4m}) \\ & + \frac{\left[9\varphi_1^2(1;\lambda) - (1+\rho)(1+\rho^{-1})\right]}{(1+\rho^{-1})}\Psi(\boldsymbol{v}^j_{4m+1})\end{aligned} \tag{40}$$

$$\begin{aligned}\Psi(\boldsymbol{v}^j_{4(m+1)}) = {} & \frac{1-9\varphi_1^2(1;\lambda)}{(1+\rho)(1+\rho^{-1})}\Psi(\boldsymbol{v}^j_{4m}) \\ & + \frac{3\varphi_1(1;\lambda)\left[9\varphi_1^2(1;\lambda) - 1 - (1+\rho)(1+\rho^{-1})\right]}{(1+\rho)(1+\rho^{-1})}\Psi(\boldsymbol{v}^j_{4m+1})\end{aligned} \tag{41}$$

$$\begin{aligned}\Psi(\boldsymbol{v}^j_{4(m+1)+1}) = {} & \frac{3\varphi_1(1;\lambda)\left[1 - 9\varphi_1^2(1;\lambda) + (1+\rho)(1+\rho^{-1})\right]}{(1+\rho)(1+\rho^{-1})}\Psi(\boldsymbol{v}^j_{4m}) \\ & + \Bigg(\frac{9\varphi_1^2(1;\lambda)\left[9\varphi_1^2(1;\lambda) - 1\right]}{(1+\rho)(1+\rho^{-1})} - 18\varphi_1^2(1;\lambda) \\ & + (1+\rho)(1+\rho^{-1})\Bigg)\Psi(\boldsymbol{v}^j_{4m+1})\end{aligned} \tag{42}$$

Analogously, $\Psi(\boldsymbol{v}^j_{4m})$, $\Psi(\boldsymbol{v}^j_{4m+1})$, $\Psi(\boldsymbol{v}^j_{4m+2})$, $\Psi(\boldsymbol{v}^j_{4m+3})$ can similarly be obtained in terms of $\Psi(\boldsymbol{v}^j_{4m})$, $\Psi(\boldsymbol{v}^j_{4m+1})$, for any arbitrary $m \in \mathbb{Z}$.

Let's fix the value of m, for example $m = 0$. From (39)–(42) we obtain $\Psi(\boldsymbol{v}^j_i)$ for all $i \geq 2$ in terms of the initial values $\Psi(\boldsymbol{v}^j_0)$, $\Psi(\boldsymbol{v}^j_1)$. In a similar way, we explicitly calculate the values of $\Psi(\boldsymbol{v}^j_i)$ for all $i \leq -1$, in terms of $\Psi(\boldsymbol{v}^j_0)$, $\Psi(\boldsymbol{v}^j_1)$. Next, it is straightforward deduced that the space of solutions has dimension 2. Thus, a base of this space are all the functions whose values at the vertices are obtained from (39)–(42), and the corresponding inverted equations for $i \leq -1$ from the initial values

$$\begin{bmatrix} \Psi(\boldsymbol{v}_0^j) \\ \\ \Psi(\boldsymbol{v}_1^j) \end{bmatrix} = \begin{bmatrix} 1 \\ \\ 0 \end{bmatrix} \quad \text{or} \quad \begin{bmatrix} \Psi(\boldsymbol{v}_0^j) \\ \\ \Psi(\boldsymbol{v}_1^j) \end{bmatrix} = \begin{bmatrix} 0 \\ \\ 1 \end{bmatrix}.$$

□

Proof of Theorem 4. Following the same notations as in the proof of the previous theorem, the solutions of $\mathcal{H}\Psi \equiv \lambda\Psi$ satisfying (27) must additionally satisfy (39)–(42), which are written in matrix form as follows:

$$\begin{bmatrix} \Psi(\boldsymbol{v}_{4(m+1)}^j) \\ \\ \Psi(\boldsymbol{v}_{4(m+1)+1}^j) \end{bmatrix} = \begin{bmatrix} M & -3\varphi_1(1;\lambda)(M+1) \\ \\ 3\varphi_1(1;\lambda)(M+1) & -9\varphi_1^2(1;\lambda)(M+2)+(1+\rho)(1+\rho^{-1}) \end{bmatrix} \begin{bmatrix} \Psi(\boldsymbol{v}_{4m}^j) \\ \\ \Psi(\boldsymbol{v}_{4m+1}^j) \end{bmatrix}$$

where

$$M = \frac{1 - 9\varphi_1^2(1;\lambda)}{(1+\rho)(1+\rho^{-1})} \tag{43}$$

Furthermore, the periodicity condition (28) implies that the vector $[\Psi(\boldsymbol{v}_{4m}^j), \Psi(\boldsymbol{v}_{4m+1}^j)]^T$ must be a non-trivial solution of the system

$$\begin{bmatrix} M-1 & -3\varphi_1(1;\lambda)(M+1) \\ \\ 3\varphi_1(1;\lambda)(M+1) & -9\varphi_1^2(1;\lambda)(M+2)+(1+\rho)(1+\rho^{-1})-1 \end{bmatrix} \begin{bmatrix} \Psi(\boldsymbol{v}_{4m}^j) \\ \\ \Psi(\boldsymbol{v}_{4m+1}^j) \end{bmatrix} = \begin{bmatrix} 0 \\ \\ 0 \end{bmatrix}. \tag{44}$$

For this problem to have non-trivial solutions, it is necessary and sufficient that

$$det \begin{bmatrix} M-1 & -3\varphi_1(1;\lambda)(M+1) \\ \\ 3\varphi_1(1;\lambda)(M+1) & -9\varphi_1^2(1;\lambda)(M+2)+(1+\rho)(1+\rho^{-1})-1 \end{bmatrix} = 0.$$

Expanding the determinant and simplifying matters, the previous equation is written equivalently as follows:

(45) $$81\varphi_1^4(1;\lambda)-18\Big[1+(1+\rho)(1+\rho^{-1})\Big]\varphi_1^2(1;\lambda)+\Big[(1+\rho)(1+\rho^{-1})-1\Big]^2=0.$$

This is a quadratic equation on the auxiliary variable

(46) $$z=(1+\rho)(1+\rho^{-1}),$$

which is explicitly written as

(47) $$z^2-2(9\varphi_1(1;\lambda)^2+1)z+(9\varphi_1(1;\lambda)^2-1)^2=0,$$

and who has real, nonnegative solutions, which are given by (29). To determine the corresponding values of ρ, we use identity(46) for each of the two solutions $z_{1,2}$, obtaining a new quadratic equation on $\rho(z)$, which is

(48) $$\rho^2+(2-z)\rho+1=0,$$

and whose solutions are given by (30). Of course, here $z=z_1$ or $z=z_2$ (see (29)).

The solutions of this equation are real and satisfy $0<\rho(z)_1<1<\rho(z)_2$ whenever $z\in(4,\infty)$. In case $z=0$, we get $\rho(z)=-1$, which has been excluded from our analysis from the beginning. In case $z=4$, we get $\rho=1$, which corresponds to periodic solutions in the horizontal direction of the lattice.

Finally, in case $z\in(0,4)$, we have complex conjugate solutions of modulus 1, so they can be written in the form

(49) $$\rho(z)_{1,2}=e^{\pm i\theta(z)},\qquad \text{where } \theta(z)=\arccos\left(\frac{z-2}{2}\right).$$

Using (29), we have

(50) $$\begin{cases} z_1\in(0,4) & \Longleftrightarrow \quad \varphi_1(1;\lambda)\in(-1,-1/3)\cup(-1/3,1/3)\\ z_1=0 & \Longleftrightarrow \quad \varphi_1(1;\lambda)=-1/3\\ z_1=4 & \Longleftrightarrow \quad \varphi_1(1;\lambda)=1/3 \quad\vee\quad \varphi_1(1;\lambda)=-1\\ z_1>4 & \Longleftrightarrow \quad \varphi_1(1;\lambda)\in(-\infty,-1)\cup(1/3,\infty)\end{cases}$$

(51) $$\begin{cases} z_2\in(0,4) & \Longleftrightarrow \quad \varphi_1(1;\lambda)\in(-1/3,1/3)\cup(1/3,1)\\ z_2=0 & \Longleftrightarrow \quad \varphi_1(1;\lambda)=1/3\\ z_2=4 & \Longleftrightarrow \quad \varphi_1(1;\lambda)=-1/3 \quad\vee\quad \varphi_1(1;\lambda)=1\\ z_2>4 & \Longleftrightarrow \quad \varphi_1(1;\lambda)\in(-\infty,-1/3)\cup(1,\infty)\end{cases}$$

Table 1 in the heading of this theorem results from summarizing the expressions (50)–(51), (49) and (30).

Next, to prove formulae (31), we start by writing the first equation of system (44) as follows

(52) $$(M-1)\Psi(\boldsymbol{v}_{4m}^j)-3\varphi_1(1;\lambda)(M+1)\Psi(\boldsymbol{v}_{4m+1}^j)=0$$

where M was defined in (43); it can be rewritten as

$$M = -\frac{(3\varphi_1(1;\lambda)+1)\,(3\varphi_1(1;\lambda)-1)}{z}. \tag{53}$$

To explicitly compute vector $[\Psi(\boldsymbol{v}^j_{4m}), \Psi(\boldsymbol{v}^j_{4m+1}), \Psi(\boldsymbol{v}^j_{4m+2}), \Psi(\boldsymbol{v}^j_{4m+3})]^T$ in terms of $\Psi(\boldsymbol{v}^j_{4m})$, we split its calculation into two cases.

i) For $\varphi_1(1;\lambda) \neq 1/3$, let's consider the case $z = z_1 = (3\varphi_1(1;\lambda)-1)^2$. If so, (53) becomes

$$M = -\frac{3\varphi_1(1;\lambda)+1}{3\varphi_1(1;\lambda)-1}$$

and hence, equation (52) is rewritten as

$$\varphi_1(1;\lambda)\left(\Psi(\boldsymbol{v}^j_{4m}) - \Psi(\boldsymbol{v}^j_{4m+1})\right) = 0. \tag{54}$$

Remark 2. It is worth noting that if $\varphi_1(1;\lambda) = 0$, then the equation (54) is satisfied for all $\Psi(\boldsymbol{v}^j_{4m}), \Psi(\boldsymbol{v}^j_{4m+1})$. For that reason, this case has not been included in this theorem.

Since $\varphi_1(1;\lambda) \neq 0$, the equation (54) becomes

$$\Psi(\boldsymbol{v}^j_{4m+1}) = \Psi(\boldsymbol{v}^j_{4m}) \tag{55}$$

To calculate $\Psi(\boldsymbol{v}^j_{4m+2})$, we use the equation (39), which by virtue of (55) reduces to

$$\Psi(\boldsymbol{v}^j_{4m+2}) = \frac{3\varphi_1(1;\lambda)-1}{(1+\rho^{-1})}\Psi(\boldsymbol{v}^j_{4m}). \tag{56}$$

To simplify this expression, let's note that using (46) and the value of $z = z_1$, we have

$$\rho = \left(\frac{3\varphi_1(1;\lambda)-1}{1+\rho^{-1}}\right)^2, \tag{57}$$

that is,

$$\frac{3\varphi_1(1;\lambda)-1}{1+\rho^{-1}} = s_1 \cdot \sqrt{\rho}, \tag{58}$$

where s_1 is given by (32). Using this identity in (56), we get

$$\Psi(\boldsymbol{v}^j_{4m+2}) = s \cdot \sqrt{\rho}\,\Psi(\boldsymbol{v}^j_{4m}). \tag{59}$$

Finally, using (55) in (40), we obtain

$$\begin{aligned}\Psi(\boldsymbol{v}^j_{4m+3}) = \frac{9\varphi_1^2(1;\lambda) - 3\varphi_1(1;\lambda) - z}{1+\rho^{-1}}\Psi(\boldsymbol{v}^j_{4m}) &= \frac{3\varphi_1(1;\lambda)-1}{1+\rho^{-1}}\Psi(\boldsymbol{v}^j_{4m}) \\ &= s \cdot \sqrt{\rho}\,\Psi(\boldsymbol{v}^j_{4m}).\end{aligned}$$

Bringing together (55), (59) with this latter expression, we obtain (31).

ii) For $\varphi_1(1;\lambda) \neq -1/3$, let's consider the case $z = z_2 = (3\varphi_1(1;\lambda)+1)^2$. If so, (53) becomes

$$M = -\frac{3\varphi_1(1;\lambda) - 1}{3\varphi_1(1;\lambda) + 1}$$

and hence, equation (52) is rewritten as

$$\varphi_1(1;\lambda)\left(\Psi(\boldsymbol{v}^j_{4m}) + \Psi(\boldsymbol{v}^j_{4m+1})\right) = 0. \tag{60}$$

Remark 3. Note that again if $\varphi_1(1;\lambda) = 0$, the equation (60) is satisfied for all $\Psi(\boldsymbol{v}^j_{4m}), \Psi(\boldsymbol{v}^j_{4m+1})$. For that reason, this case has not been considered in the theorem.

Since $\varphi_1(1:\lambda) \neq 0$, the equation (60) becomes

$$\Psi(\boldsymbol{v}^j_{4m+1}) = -\Psi(\boldsymbol{v}^j_{4m}). \tag{61}$$

Using (61) in (39), we get

$$\Psi(\boldsymbol{v}^j_{4m+2}) = -\frac{1+3\varphi_1(1;\lambda)}{1+\rho^{-1}}\Psi(\boldsymbol{v}^j_{4m}). \tag{62}$$

To simplify this expression, let's use (46) and the value of $z = z_2$, we have

$$\rho = \left(\frac{3\varphi_1(1;\lambda)+1}{1+\rho^{-1}}\right)^2, \tag{63}$$

that is,

$$\frac{3\varphi_1(1;\lambda)+1}{1+\rho^{-1}} = s_2 \cdot \sqrt{\rho}, \tag{64}$$

where s_2 is given by (32). Using this identity in (62), we get

$$\Psi(\boldsymbol{v}^j_{4m+2}) = -s\sqrt{\rho}\Psi(\boldsymbol{v}^j_{4m}). \tag{65}$$

Finally, to calculate $\Psi(\boldsymbol{v}^j_{4m+3})$ we use (40), which combined with (61), becomes

$$\begin{aligned}\Psi(\boldsymbol{v}^j_{4m+3}) = -\frac{9\varphi_1^2(1;\lambda)+3\varphi_1(1;\lambda)-z}{1+\rho^{-1}}\Psi(\boldsymbol{v}^j_{4m}) &= \frac{3\varphi_1(1;\lambda)+1}{1+\rho^{-1}}\Psi(\boldsymbol{v}^j_{4m}) \\ &= s\cdot\sqrt{\rho}\Psi(\boldsymbol{v}^j_{4m}).\end{aligned}$$

Bringing together (61), (65) with this latter expression, we obtain the second part in (31).

□

Proof of Theorem 5. Since $\varphi_2(1;\lambda) \neq 0$, Kirchhoff's conditions for solutions of $\mathcal{H}\Psi \equiv \lambda\Psi$, which satisfy (27) for $\rho = -1$, and for any profile L_j (see Figure 1), are written for each $m \in \mathbb{Z}$ as follows:

$$-3\varphi_1(1;\lambda)\Psi(\boldsymbol{v}^j_{4m}) + \Psi(\boldsymbol{v}^j_{4m+1}) = 0 \tag{66}$$

$$\Psi(\boldsymbol{v}^j_{4m}) - 3\varphi_1(1;\lambda)\Psi(\boldsymbol{v}^j_{4m+1}) = 0 \tag{67}$$

$$-3\varphi_1(1;\lambda)\Psi(\boldsymbol{v}^j_{4m+2}) + \Psi(\boldsymbol{v}^j_{4m+3}) = 0 \tag{68}$$

$$\Psi(\boldsymbol{v}^j_{4m+2}) - 3\varphi_1(1;\lambda)\Psi(\boldsymbol{v}^j_{4m+3}) = 0. \tag{69}$$

This linear system only has non-trivial solutions when $3\varphi_1(1;\lambda) = \pm 1$, in which case we obtain the solutions written in (33), (34). This completes the proof of Theorem 5. □

Acknowledgments. C. Conca is partially supported by PFBasal-001 (CeBiB) project, and from the Regional Program STIC-AmSud Project NEMBICA STIC190013, STIC-AMSud. J. San Martín received partial support from Fondecyt Grant 1180781.

REFERENCES

[1] M. J. Ablowitz, J. T. Cole, P. Hu, and P. Rosenthal, *Peierls-Nabarro barrier effect in nonlinear Floquet topological insulators.* Physical Review E **103** (2021), 042214.

[2] S. Alexander, *Superconductivity of networks. A percolation approach to the effects of disorder.* Physical Review B **27** (1983), 1541.

[3] G. Allaire and R. Orive, *On the band gap structure of Hill's equation.* Journal of Mathematical Analysis and Applications **306** (2005), 462–480.

[4] C. Amovilli, F. E. Leys, and N. H. March, *Electronic energy spectrum of two-dimensional solids and a chain of C atoms from a quantum network model.* Journal of Mathematical Chemistry **36** (2004), 93–112.

[5] J. E. Avron, A. Raveh, and B. Zur, *Adiabatic quantum transport in multiply connected systems.* Reviews of Modern Physics **60** (1988), 873.

[6] S. Becker, F. Gregorio, and D. Mugnolo, *Schrödinger and polyharmonic operators on infinite graphs: Parabolic well-posedness and p-independence of spectra.* Journal of Mathematical Analysis and Applications **495** (2021), 124748.

[7] S. Becker and M. Zworski, *Magnetic oscillations in a model of graphene.* Communications in Mathematical Physics **367** (2019), 941–989.

[8] C. Conca, J. S. Martín, and V. Solano, *A mathematical basis for the graphene.* Computational and Applied Mathematics **39** (2019), 19–52.

[9] C. Conca, R. Orive, J. S. Martín, and V. Solano, *On the graphene hamiltonian operator.* Computational and Applied Mathematics **39** (2019), 8–29.

[10] P. G. De Gennes, *Champ critique d'une boucle supraconductrice ramefieé.* C. R. Acad. Sci. Paris **292B** (1981), 279–282.

[11] M. S. Eastham, *The Spectral Theory of Periodic Differential Equations.* Scottish Academic Press Edinburgh, 1973.

[12] C. L. Fefferman and M. I. Weinstein, *Continuum Schröedinger operators for sharply terminated graphene-like structures.* Communications in Mathematical Physics **380** (2020), 853–945.

[13] J. Fillman and R. Han, *Discrete Bethe-Sommerfeld conjecture for triangular, square, and hexagonal lattices.* Journal d'Analyse Mathèmatique **142** (2020), 271–321.

[14] G. Floquet, *Sur les équations différentielles linéaires à coefficients périodiques.* Annales Scientifiques de l'École Normale Supérieure **12** (1883), 47–88.

[15] P. J. F. Harris, *Carbon nano-tubes and related structures: New materials for the twenty-first century.* AAPT, 2002.

[16] M. I. Katsnelson, *Graphene: Carbon in two dimensions.* Materials Today **10** (2007), 20–27.

[17] E. Korotyaev and I. Lobanov, *Zigzag periodic nanotube in magnetic field.* Preprint arXiv math/0604007 (2006).

[18] E. Korotyaev and I. Lobanov, *Schrödinger operators on zigzag nanotubes.* Annales Henri Poincare **8** (2007), *6*, 1151–1176.

[19] P. Kuchment and O. Post, *On the spectra of carbon nano-structures.* Communications in Mathematical Physics **275** (2007), 805–826.

[20] F. E. Leys, C. Amovilli, and N. H. March, *Topology, connectivity and electronic structure of C and B cages and the corresponding nanotubes.* Journal of Chemical Information and Computer Sciences, **44** (2004), 122–135.

[21] R. G. J. Mills and E. W. Montroll, *Quantum theory on a network. II. A solvable model which may have several bound states per node point.* Journal of Mathematical Physics **11** (1970), 2525–2538.

[22] E. W. Montroll, *Quantum theory on a network. I. A solvable model whose wave functions are elementary functions.* Journal of Mathematical Physics **11** (1970), 635–648.

[23] L. Pauling, *The diamagnetic anisotropy of aromatic molecules.* The Journal of Chemical Physics **4** (1936), 673–677.

[24] K. Ruedenberg and C. W. Scherr, *Free-electron network model for conjugated systems. I. Theory systems.* The Journal of Chemical Physics **21** (1953), 1565–1581.

[25] R. Saito, G. Dresselhaus, and M. S. Dresselhaus, *Physical Properties of Carbon Nanotubes.* World Scientific, 1998.

[26] A. Sakhnovich, *On the classes of explicit solutions of Dirac, dynamical Dirac and Dirac–Weyl systems with non-vanishing at infinity potentials, their properties and applications.* Journal of Differential Equations **275** (2021), 250–269.

C. Conca
Universidad de Chile
Mathematical Engineering Department
Center for Mathematical Modeling - UMI 2807
CNRS-UChile
and
Center for Biotechnology and Bioengineering
Beauchef 851, Santiago, Chile
cconca@dim.uchile.cl

J. San Martín
Mathematical Engineering Department and Center for Mathematical Modeling - UMI 2807 CNRS-UChile, Universidad de Chile, Beauchef 851, Santiago, Chile
jorge@dim.uchile.cl

V. Solano
Universidad de Chile
Mathematical Engineering Department
and
Center for Mathematical Modeling UMI 2807
CNRS-UChile
Beauchef 851, Santiago, Chile
and
Universidad del Desarrollo
Engineering Faculty
Avenida La Plaza 700, Santiago, Chile
vsolano@udd.cl